Journal of Colloid and Interface Science 525 (2018) 119–125

Contents lists available at ScienceDirect

Journal of Colloid and Interface Science

journal homepage: www.elsevier.com/locate/jcis

Regular Article

Effects of fibre dimension and charge density on nanocellulose gels

Llyza Mendoza, Thilina Gunawardhana, Warren Batchelor, Gil Garnier *

Bioresource Processing Research Institute of Australia (BioPRIA), Department of Chemical Engineering, Monash University, VIC 3800, Australia

GRAPHICAL ABSTRACT

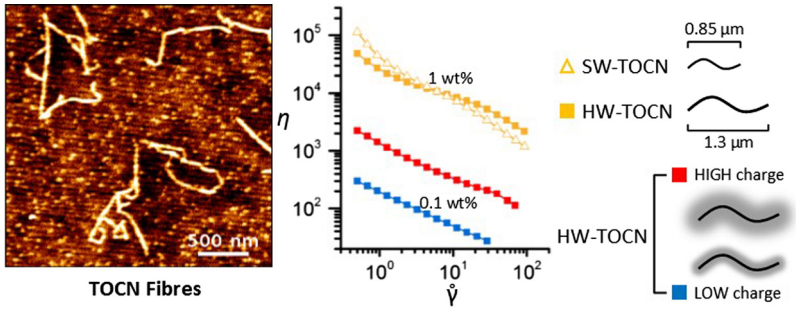

ARTICLE INFO

Article history:
Received 7 March 2018
Revised 16 April 2018
Accepted 17 April 2018
Available online 18 April 2018

Keywords:
Nanocellulose
Gel
Fibre dimension
Rheology
TEMPO-mediated oxidation
Atomic force microscopy

ABSTRACT

Hypothesis: Carboxylated cellulose nanofibres can produce gels at low concentrations. The effect of pulp source on the nanocellulose fibre dimension and gel rheology are studied. It is hypothesised that fibre length and surface charge influence aspects of the gel rheological properties.

Experiments: TEMPO (2,2,6,6-tetramethylpiperidine-1-oxyl)- mediated oxidised cellulose nanofibres from never-dried hardwood and softwood pulp and containing different charge levels were produced and characterized. Steady-state and dynamic rheological studies were performed to ascertain the effects of pulp type on gel behavior and properties.

Findings: Nanocellulose fibres extracted from softwood (SW-TOCN) and hardwood (HW-TOCN) pulp exhibit similar widths but different length dimensions as shown via AFM analysis. Rheological measurements show that the dynamic moduli (G′ and G″) of nanocellulose gels are independent of pulp source and are mostly influenced by fibre concentration. Differences in the steady-state behavior (i.e. viscosity) at constant surface charge can be attributed to differences in fibre length. Increasing the surface charge density influences the critical strain and the viscosity at the percolation concentration (0.1 wt%) due to higher electrostatic interactions.

1. Introduction

Cellulose nanofibres are long semi-flexible fibrils derived from the disintegration of wood pulp via various chemical and mechanical treatments [1]. Chemical methods, such as TEMPO-mediated oxidation, selectively introduce carboxylate moieties on the cellulose fibril surface. The high electrostatic repulsion between the individual fibrils assists in the liberation of TEMPO-oxidised cellulose nanofibres (TOCNs) upon mechanical disintegration [2]. The ease of scale-up of TEMPO-mediated oxidation has led to the establishment of pilot-scale production and its availability as a commercial product [3]. Applications of TOCNs extend far beyond pulp and paper. TOCNs have shown great performance as reinforcing agent in plastics, [4,5], in biomedical applications [6–11], pharmaceuticals [12], catalysis [13], superabsorbents [14,15], and flexible electronics [16].

* Corresponding author.
E-mail address: gil.garnier@monash.edu (G. Garnier).

https://doi.org/10.1016/j.jcis.2018.04.077
0021-9797/

Nanocellulose is typically found as a suspension or a gel with water as continuous phase. Rheology is the technique of choice to quantify nanocellulose behavior and properties. For instance, the flow behavior of semi-flexible nanocellulose fibrils can be related to the length and width of the fibrils. The studies of Tanaka et al. [17] and Jowkarderis and van de Ven [18], related shear and intrinsic viscosities of dilute TOCN suspensions to equations of flow for rigid rod-like particles to determine fibre aspect ratio. Varanasi et al. [19], on the other hand, utilised yield stress measurements to determine the fibre gel point and correlate it to the aspect ratio via the crowding factor theory.

The bulk properties of nanocellulose gels and suspensions have been investigated in several rheological studies. In particular, TOCNs possess high aspect ratio [2] which form percolated networks even at low solid concentrations [20]. TOCNs and similarly surface-charged nanocellulose suspensions form gels which exhibit pseudoplastic and thixotropic behavior due to their inherent fibril assembly and restructuring which occurs during material deformation [20–22]. The presence of high surface charges leading to their colloidal stability was also investigated in several studies [20,23–25]. Local flow phenomenon in nanocellulose such as wall slip, shear-banding, and other flow instabilities which may affect the accuracy of rheological measurements were analysed [12,21]. Simulation and numerical modelling have mainly focused on understanding the mechanism of shear-thinning in nanocellulose [26,27]. However, studies on the effects of fibre dimensions and surface charges, on the nanocellulose gel rheological properties are very limited. Only one known study has related nanocellulose aspect ratio to the changes in the fibre percolation as observed by changes in viscosity [28].

This study aims at quantifying the effect of fibre dimension and surface charge on the rheological properties of nanocellulose gels. Fibre dimension was varied with the pulp source by oxidising softwood and hardwood kraft pulp from *Pinus Radiata* and *Eucalyptus* sp. respectively. The objectives are two-fold. First, to understand the relationship between the initial fibre size on the dimensions of the resulting nanocellulose; second to quantify the effect of nanocellulose fibre dimension on gel rheology. Differences are analysed through steady-state shear and oscillatory rheological measurements via cone and plate geometry. In steady-state shear, changes in the signature double yielding-behavior and zero-shear viscosity will be observed, whereas in oscillatory measurements variations in the key parameters such as the dynamic (G' and G'') moduli and the critical strain γ_c are examined.

2. Methodology

2.1. Materials

Hardwood (*Eucalyptus* sp.) kraft pulp of approximately 10 wt% solids was supplied by Australian Paper, Maryvale, Australia. Softwood (*Pinus Radiata*) kraft pulp containing 17.7 wt% solids was supplied by Oji Fibre Solutions, Kinleith, New Zealand. 2,2,6,6-tetra methylpiperidine-1-oxyl (TEMPO) and sodium bromide (NaBr) were purchased from Sigma-Aldrich. Hydrochloric acid (HCl) and Sodium Hydroxide (NaOH) were diluted for solutions as required and were purchased from ACL Laboratories and Merck, respectively. 12 w/v% Sodium Hypochlorite (NaClO) was purchased from Thermo Fisher Scientific and used as received. All chemicals were analytical grade.

2.2. TEMPO-mediated oxidation

The TEMPO-mediated oxidation process employed is based on the method of Isogai et al. [2]. Wood pulp containing 10 dry g fibre was suspended in 2500 mL water containing 0.4 g TEMPO and 2.5 g NaBr. The 12 w/v% NaClO solution was initially adjusted to pH 10 via addition of 36% HCl before the reaction. To initiate the oxidation process, NaClO was added drop-wise to the suspension whilst stirred. Varying amounts of NaClO was added depending on the desired carboxylate group density. The primary oxidant content was varied between 3.3 mmol $NaClO{\cdot}g^{-1}$ fibre to 12.5 mmol $NaClO{\cdot}g^{-1}$ fibre for hardwood and constant 6.5 mmol $NaClO{\cdot}g^{-1}$ fibre for softwood. The pH of the reaction was maintained at 10 through the addition of 0.5 M NaOH. The oxidation process was maintained until no pH change was observed. The oxidised fibres were recovered through filtration and stored refrigerated (4 °C). The oxidised pulp was then dispersed in deionised water to a desired concentration (0.1–1 wt%). Fibrillation was accomplished through a high-pressure homogeniser (GEA Niro Soavi Homogerniser Panda) at 1000 bar for two passes.

2.3. Determining solids concentration

The solids concentration of all samples (i.e. gel or pulp) were determined through drying. The sample was weighed before (w_i) and after (w_d) drying. Sample moisture was evaporated by drying in an oven at 105° for at least 6 h. The solids content was calculated as:

$$solidscontent(\%) = \frac{w_d}{w_i} \times 100\% \quad (1)$$

2.4. Conductometric titration

The carboxylate group content was measured by conductometric titration as reported in [29]. Oxidised pulp samples (approx. 30 mg dry weight) were suspended in 40 mL deionised water. 40 μL 1% NaCl was added to the suspended sample. The pH of the suspended sample was adjusted between 2.5 and 3 prior to titration with 0.5 M HCl. Titration was accomplished by controlled addition of 0.1 M NaOH using a Mettler Toledo T5 titrator. The conductivity of the sample was monitored throughout the titration progress. The carboxyl group content (mmol $COO^-Na^+ .g^{-1}$ fibre) was determined with:

$$CC = \frac{c(V_2 - V_1)}{w} \times 1000 \quad (2)$$

where V_1 and V_2 pertain to the amount of titrant required to neutralise the carboxylic groups (in L), c is the NaOH concentration (mol/L), and w is the sample weight (g).

2.5. Rheological measurement

Rheological testing was performed with an Anton Paar MCR302 rheometer. A cone (0.997°) and plate (49.975 mm) geometry were selected. Testing was done at ambient temperature (25 °C). A solvent trap was used to ensure stable temperature during measurements. Viscosity was measured at shear rate ranging from 0.5 to 100 s^{-1}. Oscillatory strain sweep was performed from 0.01 to 100% at a constant 1 Hz frequency. Frequency sweep was measured from 0.1 to 100 rad/s and at various suitable shear stresses at the linear viscoelastic region (LVR) wherein the dynamic moduli (G' and G'') are independent of the shear stress. All measurements were done in triplicates and the most representative result is presented.

2.6. Atomic force microscopy (AFM)

AFM imaging was performed using a JPK Nanowizard 3 to determine fibre length and width. A 0.001 wt% nanocellulose dispersion

was spin coated (Laurell technologies, WS-400BZ-6NPP/LITE) at 2500 rpm onto a plasma coated glass slide. Images were obtained in intermittent contact mode using Brüker NCHV model cantilevers. Fibre widths were obtained from the reported height of single fibres on the surface due to convolution effects. Fibre lengths were estimated by placing segmented lines on the AFM images through an imaging software (Fiji).

2.7. Fibrelab

Fibre dimensions (length and width) of the unrefined and unoxidised hardwood and softwood samples have been obtained via the Kajaani Fibre Lab (Valmet). Dilute suspensions (~0.05 wt%) were utilised for size analysis. Image analysis from the Fibrelab software is primarily capable of detecting large fibres more than fines.

3. Results

The effect of fibre dimensions, using never-dried bleached kraft pulp of softwood and hardwood, on the dimensions and charge density of cellulose nanofibres resulting from TEMPO- mediated oxidation pre-treatment and homogenization is first studied. Secondly, the rheological properties of the gel formed are quantified to understand the effect of nanocellulose dimensions and surface charge (i.e. extent of oxidation).

3.1. Fibre dimensions

The distributions of fibre length and width of never-dried unrefined softwood and hardwood kraft pulps are shown in Fig. 1. On average, hardwood pulp has shorter and narrower fibres than softwood; length and width distributions are also much narrower (Tables 1 and 2). However, the fibre average aspect ratio (*L/W*) are nearly identical for both fibres, with hardwood *L/W* = 36 and softwood *L/W* = 42.

The fibre size distributions of TEMPO-oxidised cellulose nanofibres produced from hardwood (HW-TOCN) and softwood (SW-TOCN) pulp containing different surface charges are shown in Fig. 2. The nanocellulose produced in all cases have the width distribution in the nano-scale- as expected from TEMPO-mediated oxidation. Length distributions, on the other hand, have changed post- chemical oxidation and mechanical fibrillation. For both fibre types and their varying surface charge levels, the mean length decreased drastically as shown in Tables 1 and 2. On average, hardwood-nanocellulose (HW-TOCN) are wider and longer than softwood-nanocellulose (SW-TOCN) at similar surface charge (1 mmol $COO^{-}\cdot g^{-1}$ fibre) as shown in Tables 1 and 2. Moreover, length and width distributions for HW-TOCNs are slightly broader than for SW-TOCNs. When surface charge is modified in HW-TOCNs, length and width dimension distributions and mean values are very similar.

3.2. Rheological measurements

Oscillatory rheology is an ideal technique to characterize the elastic and viscous behavior of nanocellulose gels at varying conditions. For instance, the rheology of nanocellulose gels produced from softwood pulp at increasing fibre concentration is shown in Fig. 3. The elastic modulus G' pertains to the solid-like behavior whereas the viscous modulus G'' characterizes the liquid-like behavior of the gel. At the linear viscoelastic region (LVR), G′ and G″ are independent of the shear strain. When G′ > G″, the elastic behavior of the nanocellulose gel is dominant at a particular strain. At the critical strain γ_c, the gel moduli (G' and G'') deviates from the LVR and is at the onset of yielding. Consequently, at even higher strains when $G'' > G'$, the gel possesses a viscous dominant behavior.

3.2.1. Effect of pulp source

The effect of initial pulp source on the dynamic moduli (G' and G'') at various solid concentrations is shown in Fig. 4A. At constant charge density (1 mmol $COO^{-}\cdot g^{-1}$ fibre), the elastic moduli (G′) of nanocellulose gels derived from hardwood and softwood sources are very similar. The differences in the viscous moduli (G″) observed between HW-TOCN and SW-TOCN are within the error margins. Moreover, for both types of pulp, γ_c is constant across all solids contents as shown in Fig. 4B. However, SW-TOCN possess consistently higher γ_c at all tested concentrations.

The difference of pulp source on the resultant nanocellulose gels viscosity profile is highlighted in Fig. 5. SW-TOCN and HW-TOCN both display similar viscosity values and linear shear-thinning behavior at 0.1 wt%. On the other hand, the double yielding behavior is observed for HW-TOCN and SW-TOCN at concentrations equal or greater than 0.3 wt%. The major difference in nanocellulose produced from hardwood and softwood pulp sources is emphasized at the semi-dilute concentrations (0.3–1 wt%) wherein SW-TOCN viscosity decreases at a steeper gradient at both double yielding regions than HW-TOCNs.

3.2.2. Effect of charge density

The effect of charge density on the dynamic rheological properties of nanocellulose gels produced from hardwood is shown in Fig. 6. Gels with the lowest carboxylate content (0.65 mmol·g^{-1}) consistently report the lowest G' and G'' values. However, gels

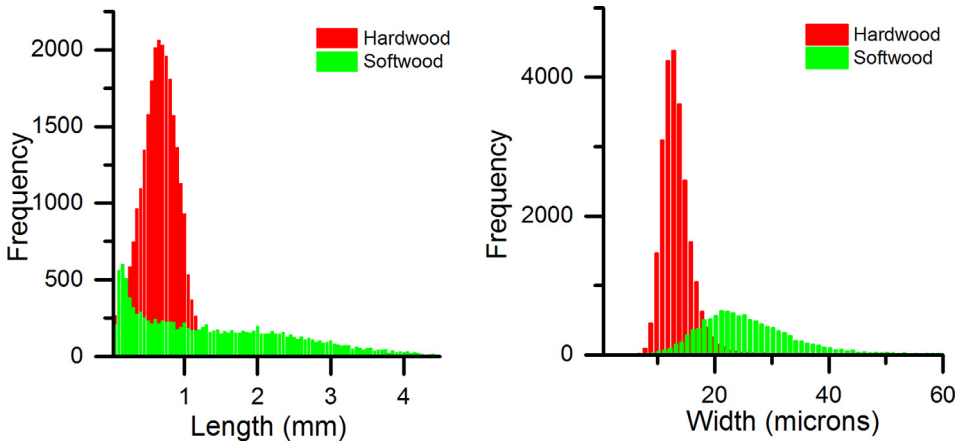

Fig. 1. Population Length and width distributions for hardwood and softwood bleached kraft pulp fibres.

Table 1
Fibre length statistics of hardwood and softwood kraft pulp and the nanocellulose fibres produced from those.

Pulp type	Surface charge (mmol $COO^{-}.g^{-1}$)	Mean length (μm)	Standard deviation (μm)	Population (# of fibres)
Hardwood	0	620	260	26,327
HW – TOCN	0.65	1.16	0.62	105
	1.00	1.30	0.73	111
	1.40	1.02	0.53	103
Softwood	0	1420	1130	13,070
SW-TOCN	1.00	0.85	0.42	99

Table 2
Fibre width statistics of hardwood and softwood bleached kraft pulp and the nanocellulose fibres produced from those.

Pulp source	Surface charge (mmol $COO^{-}.g^{-1}$)	Mean width (nm)	Standard deviation (nm)	Population (# of fibres)
Hardwood	0	17,240	4253	24,441
HW – TOCN	0.65	1.06	0.37	105
	1.00	1.24	0.33	111
	1.40	1.29	0.47	103
Softwood	0	34,060	9028	10,799
SW-TOCN	1.00	0.97	0.30	99

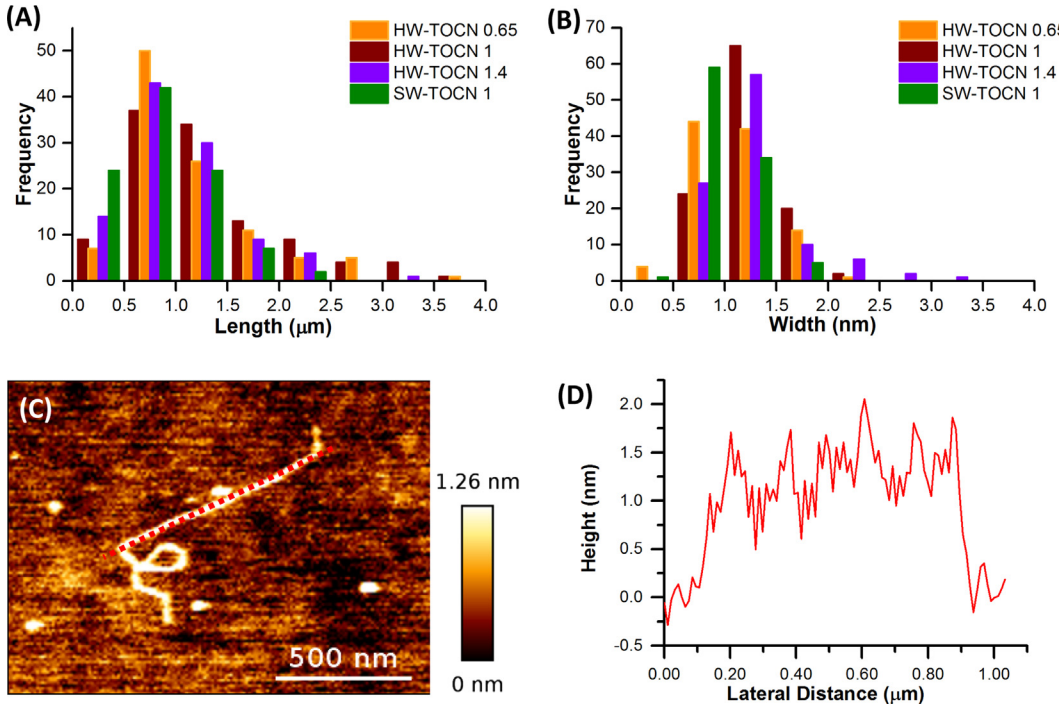

Fig. 2. Nanocellulose fibres produced from softwood and hardwood bleached kraft pulp. Width (A) and length (B) distributions for nanocellulose produced from softwood (1mmol $COO^{-}.g^{-1}$) and hardwood (0.65, 1, and 1.4 mmol.g^{-1}) at various surface charges. (C) and (D) AFM image of a single HW-TOCN fibre with surface topology shown.

containing either 1 or 1.4 mmol·g^{-1} show similar G'. On the other hand, G'' values were also observed to increase with increasing carboxylate content at all solids concentrations. Critical strain γ_c does not vary significantly up to a charge density of 1 mmol·g^{-1}. At the highest surface charge tested (1.4 mmol·g^{-1}), γ_c decreases linearly with increasing fibre content.

The viscosity profile of nanocellulose gels produced from hardwood at different surface charges is shown in Fig. 7. All HW-TOCN gels containing at least 0.3 wt% possess a double yielding behavior. At a given concentration past 0.3 wt%, the differences in the absolute viscosity values are minimal and could be attributed to small variations in actual nanocellulose content in the tested samples. However, at 0.1 wt%, the gel containing the lowest surface charge at 0.65 mmol·g^{-1} is significantly less viscous than at 1 and 1.4 mmol·g^{-1}.

4. Discussion

4.1. Effect of pulp fibres on nanocellulose fibre dimensions

Cellulose fibres vary in fibre dimension and chemical composition depending on the original wood source and the pulping process used. The most widely-used process to produce cellulosic fibres is through a combination of kraft chemical pulping followed by bleaching. This process removes most of the lignin and hemicellulose that occur in different amounts and compositions in softwood (*Pinus Radiata*), and hardwood (*Eucalyptus* sp.) [30,31]. However, traces of lignin and hemicellulose still remain within the bleached cellulose pulp which impact the TEMPO-mediated oxidation process. The softwood pulp used in this study required a higher primary oxidant content (6.5 mmol NaClO·g^{-1} fibre) than

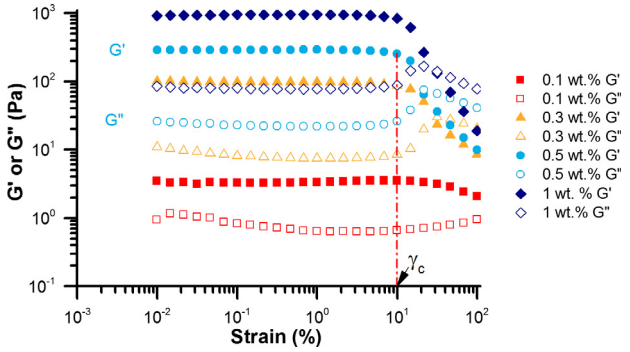

Fig. 3. Oscillatory strain measurement for nanocellulose gels made from bleached softwood fibres (1 mmol.g^{-1}) as a function of solids concentration. Important spectral rheological data including the G′ and G″ at the linear viscoelastic region (LVR), and the critical strain γ_c are identified for the 0.5 wt% gel used as example. Measurements were done at 25 °C, 1 Hz.

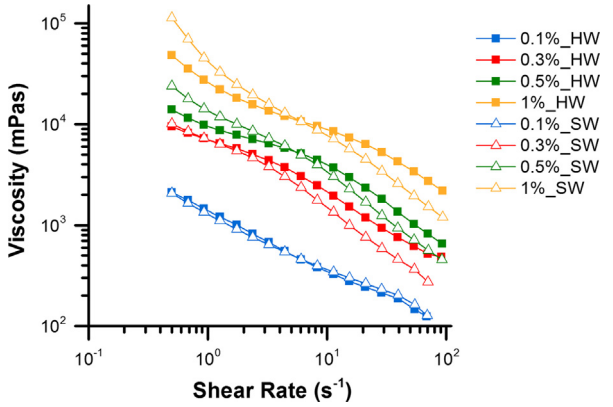

Fig. 5. Viscosity Profile of TOCNs from hardwood (solid symbol) and softwood (open symbol) as a function of concentration for constant charge density (1 mmol. g^{-1}). Measurements were done at 25 °C.

the hardwood pulp (5 mmol NaClO·g^{-1} fibre) to achieve the same surface charge (1 mmol COO$^-$.g^{-1} fibre).

The original width and length of the never-dried bleached hardwood and softwood fibres are vastly different (Fig. 1) – softwood fibres are approximately twice as long and thick on average compared to hardwood fibres (Tables 1 and 2). The combination of TEMPO-mediated oxidation and high-pressure homogenisation results in nanocellulose fibres with dimensions multiple orders of magnitude smaller. This chemical and mechanical treatment has effectively liberated elementary fibrils from both hardwood and softwood pulp sources, evident by the similar widths of the HW-TOCN and SW-TOCN fibres in the order of nanometers [15]. Due to the high energy required for mechanical fibrillation (i.e. 1000 bar pressure), it is possible that further delamination occurred resulting in a fibre mean width less than the currently accepted elementary fibril dimensions consisting a 6 × 6 chain array. Since individual cellulose chains are assembled into fibrils by H-bonding along their length, the high-pressure homogenisation could have created shear forces strong enough to liberate thinner fibrils. The widths measured support previous studies. For instance, Usov et al. [32] reported AFM measurements visualising single cellulose chains and 2 × 2 cellulose nanofibrils with average widths of 0.44 and 0.84 nm, respectively. In addition, Geng et al. [33] described a mean width value of 2.35 nm (at a surface charge of 980 μmol·g^{-1}); however, width distributions showed a large proportion of fibres thinner than 2 nm. When comparing lengths of the HW-TOCN and SW-TOCN fibres, cleavage is evident for both pulp sources, attributed to the preferential oxidation of the weak amorphous regions subsequently cleaved under intense mechanical fibrillation [34]. This is evident in the XRD spectra (Supporting Information) as the small reduction in the crystalline index (CI) could not account for the large degree of fibrillation which we have observed. On average, the resulting HW-TOCNs are longer than SW-TOCNs (1.30 μm versus 0.85 μm) for a surface charge of 1 mmol COO$^-$·g^{-1}.

4.2. Effect of nanofibre dimensions and surface charge on gel rheology

TEMPO-oxidised nanocellulose are characterized by two key parameters: physical dimensions (length and width) and surface charge. For TOCNs, provided sufficient electrostatic repulsion and mechanical fibrillation, width is determined by the elementary fibril width which is similar for hardwood and softwood pulp [35]. Length, on the other hand, can vary depending on the processing conditions [2]. The change in length of a semi-flexible fibre affects the extent and ability of entanglement. For SW-TOCN and HW-TOCN, the difference in fibre lengths is most evident at the onset (i.e. critical strain values) of yielding and steady-state shear (i.e. viscosity) behavior. Across all concentrations, the shorter SW-TOCNs consistently yielded at higher strains than HW-TOCNs. This might be due to a longer persistence length, related to the flexibility and stiffness of the crystalline domains of softwood, affecting nanofibre conformation upon shear [32].

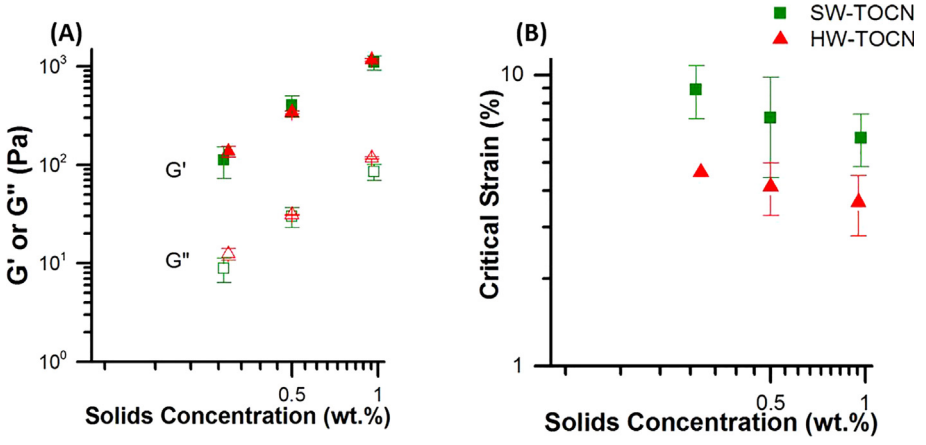

Fig. 4. (A) Dynamic Moduli (G′ and G″) of nanocellulose gels produced from unrefined softwood and hardwood as a function of solids concentration at constant charge density (1 mmol.g^{-1}). (B) Critical Strain of SW-TOCN and HW-TOCN as a function of solids concentration.

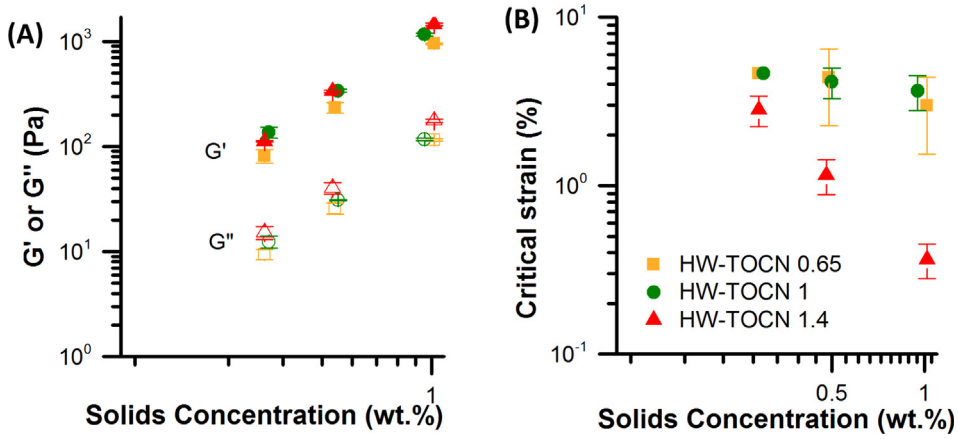

Fig. 6. The effect of charge density on the (A) dynamic moduli at LVR and (B) critical strain of HW-TOCN nanocellulose gels at different solids concentrations. Yellow symbols for 0.65 mmol.g^{-1}, green symobols for 1 mmol.g^{-1} and red symbols for 1.4 mmol.g^{-1}. Measurements were done at 25 °C, 1 Hz.

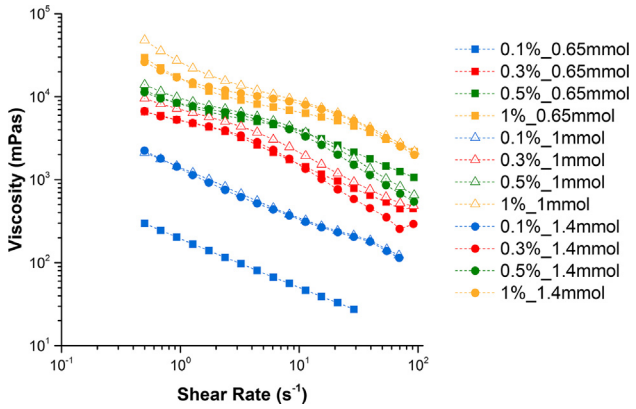

Fig. 7. Viscosity Profile for HW-TOCNs at three levels of charge density (0.65, 1, and 1.4 mmol.g^{-1}) and different solids content. Measurements were done at 25 °C.

Nanocellulose gels exhibit shear-thinning response which is generally understood to be due to the alignment of fibres along the shear direction. As seen in Fig. 5, for concentrations ranging between 0.3 and 1 wt%, SW-TOCNs have steeper viscosity gradients than HW-TOCNs due to easier alignment of the shorter fibres. However, this difference does not seem to affect the percolation threshold which is identified as the concentration wherein there is no double yielding behavior [20]. The double-yielding phenomenon in nanocellulose is attributed to the reorientation of fibres from an isotropic (i.e. randomly oriented) state to partial alignment in the direction of flow. At high fibre concentrations, higher shear rates are required to disrupt any remaining isotropic micro-domains, which leads to a further decrease in viscosity [36]. For both softwood and hardwood-based nanocellulose, the percolation concentration is 0.1 wt%. Moreover, the dynamic moduli in the LVR region are not significantly different from both pulp types and are primarily concentration-dependent (Fig. 4A).

Effective surface charge arising from the nanocellulose carboxylate groups dictates the colloidal stability of the gels [20]. HW-TOCN gel with the lowest charge density (0.65 mmol.g^{-1}) has lower moduli than HW-TOCN gels of higher charge density (Fig. 6A). A higher surface charge creates stronger and more stable gels due to higher electrostatic repulsion. The gel critical strain is affected by the variation in the surface charges (Fig. 6B). At 1.4 mmol.g^{-1}, the critical strain decreases at increasing concentration. This is not a direct effect of the fibre dimensions as we should observe some differences between 0.65 mmol·g^{-1} and 1 mmol·g^{-1}. The observations at 1.4 mmol·g^{-1} can be attributed to the repulsive charges among fibres which act as lubricant allowing fibres to slide past each other [37]. Hence, the combination of high surface charge and high fibre concentration results in stronger repelling, partially hydrated fibres per unit volume, which reduces the required minimum strain for yielding. Comparing three levels of carboxylation (Fig. 7) reveals a significant impact on viscosity at the percolation threshold. At 0.1 wt% concentration, the reduction in the surface charge to 0.65 mmol·g^{-1} results in an order of magnitude reduction in gel viscosity, possibly due to the less constrained nature of the fibre interactions. A fibre containing low surface charge is expected to have less interactions with other neighbouring fibres as it has a lower effective electrical double layer.

5. Conclusion

TEMPO-oxidised cellulose nanofibres (TOCNs) are semi-flexible fibrils derived from the primary alcohol oxidation of cellulose-based sources. Previous studies have primarily focussed on integrating TOCNs into other compatible materials to improve their bulk properties [4,5,10,14]. Some fundamental studies have been conducted, aiming to understand the colloidal stability [20,23], local flow phenomenon [12,21], and model rheological behavior [26,27]. The effect of different process conditions (i.e. bleach content and pH, primary oxidant) have been explored previously [2,38,39], however little is known on how the fibre source and its dimensions affect the rheological properties of nanocellulose gels. This study analysed the effect of wood pulp source and the resulting nanocellulose fibre dimensions on the rheology of nanocellulose gels. Kraft pulped and bleached hardwood (*Eucalyptus* sp.) and softwood (*Pinus Radiata*) contained fibres with significantly different dimensions (L = 0.6 mm, W = 17 μm and L = 1.4 mm, W = 34 μm, respectively) but similar aspect ratios (36 and 42 respectively). However, the initial fibre size has minimal effect on the degree of fibrillation, resulting in hardwood and softwood nanocellulose fibers (HW-TOCN and SW-TOCN) with similar widths in the order of nanometers, indicating elementary fibrils. In terms of length, HW-TOCN fibres are longer than SW-TOCN (L = 1.3 μm and L = 0.9 μm, respectively). The decrease in length from initial macro-fibres for both pulp sources is attributed to the preferential oxidation at weak amorphous regions cleaved under intense mechanical fibrillation. This difference in length affects the onset of yielding (ie. critical strain) and the evolution of the viscosity curves at increasing solids content. This is particularly evident via rheology at the semi-dilute concentrations (0.3–1 wt%) – shorter SW-TOCN fibres display a steeper viscosity gradient in con-

trast to HW-TOCNs. Surface charge also impacts the rheological properties at the percolation threshold – for 0.1 wt% HW-TOCN, increasing the surface charge from 0.65 to at least 1 $mmol \cdot g^{-1}$ results in higher viscosity due to greater electrostatic interactions. However, at higher concentrations, fibre length and surface charge have minimal effect, and instead the gel dynamic rheological properties (G' and G'') are primarily affected by fibre concentration. These results indicate that, at fibre concentrations greater than the percolation threshold, nanocellulose gels can be produced with similar properties regardless of pulp source and minimal surface charge. This is a key finding beneficial for engineering nanocellulose gels for any specific biomedical or rheology application.

Acknowledgments

This work was funded by the ARC Bioprocessing Advance Manufacturing Industry Research Transformation (BAMI) Hub IH13100016, Visy, Norske Skog, Orora, CHH/Oji Paper, Australian Paper and Circa. Many thanks to Australian Paper and Oji Fibre Solutions for providing the pulp. Paul Banham (Norske Skog) for Fibrelab results. Dr. Rico Tabor for his insightful discussion about colloids and rheology. Dr. Vikram Raghuwanshi and Dr. Jisheng Ma (Monash X-ray Platform) for their assistance in performing XRD measurements. This research used equipment (Bruker D8 Discover) funded by Australian Research Council grant LE130100072.

Appendix A. Supplementary material

Supplementary data associated with this article can be found, in the online version, at https://doi.org/10.1016/j.jcis.2018.04.077.

References

[1] N. Quennouz et al., Rheology of cellulose nanofibrils in the presence of surfactants, Soft Matter 12 (1) (2016) 157–164.
[2] A. Isogai, T. Saito, H. Fukuzumi, TEMPO-oxidized cellulose nanofibers, Nanoscale 3 (1) (2011) 71–85.
[3] R.S. Reiner, A.W. Rudie, Experiences with scaling-up production of TEMPO-grade cellulose nanofibrils, in: Nanocelluloses: Their Preparation, Properties, and Applications, American Chemical Society, 2017, pp. 227–245.
[4] S. Fujisawa et al., Superior reinforcement effect of TEMPO-oxidized cellulose nanofibrils in polystyrene matrix: optical, thermal, and mechanical studies, Biomacromolecules 13 (7) (2012) 2188–2194.
[5] M. Bulota, M. Hughes, Toughening mechanisms in poly(lactic) acid reinforced with TEMPO-oxidized cellulose, J. Mater. Sci. 47 (14) (2012) 5517–5523.
[6] S. Morimune-Moriya et al., Hydroxyapatite formation on oxidized cellulose nanofibers in a solution mimicking body fluid, Polym. J. 47 (2) (2015) 158–163.
[7] J. Cheng, M. Park, J. Hyun, Thermoresponsive hybrid hydrogel of oxidized nanocellulose using a polypeptide crosslinker, Cellulose 21 (3) (2014) 1699–1708.
[8] N.E. Zander et al., Metal cation cross-linked nanocellulose hydrogels as tissue engineering substrates, ACS Appl. Mater. Interfaces 6 (21) (2014) 18502–18510.
[9] J. Feng et al., Antimicrobial activity of silver nanoparticles in situ growth on TEMPO-mediated oxidized bacterial cellulose, Cellulose 21 (6) (2014) 4557–4567.
[10] S.-S. Kim et al., High-Fidelity bioelectronic muscular actuator based on graphene-mediated and TEMPO-oxidized bacterial cellulose, Adv. Funct. Mater. 25 (23) (2015) 3560–3570.
[11] A. Shimotoyodome et al., Regulation of postprandial blood metabolic variables by TEMPO-oxidized cellulose nanofibers, Biomacromolecules 12 (10) (2011) 3812–3818.
[12] O. Nechyporchuk, M.N. Belgacem, F. Pignon, Concentration effect of TEMPO-oxidized nanofibrillated cellulose aqueous suspensions on the flow instabilities and small-angle X-ray scattering structural characterization, Cellulose 22 (4) (2015) 2197–2210.
[13] A. Azetsu et al., Direct synthesis of gold nanocatalysts on TEMPO-oxidized pulp paper containing aldehyde groups, 8 (2013).
[14] N. Isobe et al., TEMPO-oxidized cellulose hydrogel as a high-capacity and reusable heavy metal ion adsorbent, J. Hazard. Mater. 260 (2013) 195–201.
[15] F. Jiang, Y.-L. Hsieh, Super water absorbing and shape memory nanocellulose aerogels from TEMPO-oxidized cellulose nanofibrils via cyclic freezing-thawing, J. Mater. Chem. A 2 (2) (2014) 350–359.
[16] H. Koga et al., Transparent, conductive, and printable composites consisting of TEMPO-oxidized nanocellulose and carbon nanotube, Biomacromolecules 14 (4) (2013) 1160–1165.
[17] R. Tanaka et al., Influence of flexibility and dimensions of nanocelluloses on the flow properties of their aqueous dispersions, Biomacromolecules 16 (7) (2015) 2127–2131.
[18] L. Jowkarderis, T.G.M. van de Ven, Intrinsic viscosity of aqueous suspensions of cellulose nanofibrils, Cellulose 21 (4) (2014) 2511–2517.
[19] S. Varanasi, R. He, W. Batchelor, Estimation of cellulose nanofibre aspect ratio from measurements of fibre suspension gel point, Cellulose 20 (4) (2013) 1885–1896.
[20] L. Mendoza et al., Gelation mechanism of cellulose nanofibre gels: a colloids and interfacial perspective, J. Colloid Interface Sci. 509 (2018) 39–46.
[21] B. Nazari et al., Rheology of cellulose nanofibers suspensions: boundary driven flow, J. Rheol. 60 (6) (2016) 1151–1159.
[22] M. Iotti et al., Rheological Studies of microfibrillar cellulose water dispersions, J. Polym. Environ. 19 (1) (2011) 137–145.
[23] M. Nordenström et al., Formation of colloidal nanocellulose glasses and gels, Langmuir 33 (38) (2017) 9772–9780.
[24] F. Martoia et al., Micro-mechanics of electrostatically stabilized suspensions of cellulose nanofibrils under steady state shear flow, Soft Matter 12 (6) (2016) 1721–1735.
[25] L. Jowkarderis, T.G.M. van de Ven, Rheology of semi-dilute suspensions of carboxylated cellulose nanofibrils, Carbohydr. Polym. 123 (2015) 416–423.
[26] A. Puisto et al., Modeling the rheology of nanocellulose suspensions, Nord. Pulp Pap. Res. J. 27 (2) (2012) 277–281.
[27] A. Puisto et al., Modeling the viscosity and aggregation of suspensions of highly anisotropic nanoparticles, Eur. Phys. J. E 35 (1) (2012) 6.
[28] T. Moberg et al., Rheological properties of nanocellulose suspensions: effects of fibril/particle dimensions and surface characteristics, Cellulose 24 (6) (2017) 2499–2510.
[29] D. da Silva Perez, S. Montanari, M.R. Vignon, TEMPO-mediated oxidation of cellulose III, Biomacromolecules 4 (5) (2003) 1417–1425.
[30] P. Martínez, M. Pereira, R.T. Mendonça, Retention and structure of xylans from eucalyptus globulus genotypes with different pulpwood characteristics, J. Wood Chem. Technol. 35 (2) (2015) 129–136.
[31] N. Cruz et al., Impact of the chemical composition of pinus radiata wood on its physical and mechanical properties following thermo-hygromechanical densification. 13 (2018).
[32] I. Usov et al., Understanding nanocellulose chirality and structure–properties relationship at the single fibril level, Nat. Commun. 6 (2015) 7564.
[33] L. Geng et al., Understanding the mechanistic behavior of highly charged cellulose nanofibers in aqueous systems, Macromolecules 51 (4) (2018) 1498–1506.
[34] R. Zimmermann et al., Oxidation and structural changes in NMMO-regenerated cellulose films, Cellulose 23 (6) (2016) 3535–3541.
[35] G. Chinga-Carrasco, Y. Yu, O. Diserud, Quantitative electron microscopy of cellulose nanofibril structures from eucalyptus and pinus radiata kraft pulp fibers, Microsc. Microanal. 17 (4) (2011) 563–571.
[36] E. Lasseuguette, D. Roux, Y. Nishiyama, Rheological properties of microfibrillar suspension of TEMPO-oxidized pulp, Cellulose 15 (3) (2008) 425–433.
[37] M.A. Hubbe et al., Rheology of Nanocellulose-rich Aqueous Suspensions: A Review. 12 (2017)
[38] A.E.J. de Nooy, A.C. Besemer, H. van Bekkum, Highly selective tempo mediated oxidation of primary alcohol groups in polysaccharides, Recl. Trav. Chim. Pays-Bas 113 (3) (1994) 165–166.
[39] K. Benhamou et al., Control of size and viscoelastic properties of nanofibrillated cellulose from palm tree by varying the TEMPO-mediated oxidation time, Carbohydr. Polym. 99 (Supplement C) (2014) 74–83.